Computational Materials Science 79 (2013) 110–117

Contents lists available at SciVerse ScienceDirect

Computational Materials Science

journal homepage: www.elsevier.com/locate/commatsci

The structure and mechanical properties in amorphous alumina under pressure

Van-Vinh Le *, Viet-Huy Nguyen, Van-Hong Nguyen, Khac-Hung Pham

Department of Computational Physics, Hanoi University of Science and Technology, No. 1 Dai Co Viet, Hanoi, Viet Nam

ARTICLE INFO

Article history:
Received 10 April 2013
Received in revised form 29 May 2013
Accepted 1 June 2013
Available online 5 July 2013

Keywords:
Simulation
Amorphous alumina
Bond angle
Coordination number
Deformation

ABSTRACT

Molecular dynamics simulations of amorphous alumina with various densities ranged from 2.84 to 3.81 g cm^{-3} were carried out to investigate their local atomic configuration and mechanical properties. The local atomic structure was analyzed through the pair radial distribution functions, bond angle distributions and simplex statistics. The simulation reveals that a mathematic expression can be derived from a relationship between bond angle distribution and structural units AlO_x (and linkages OAl_y). The density can be estimated through the fraction of structural units AlO_x. Void volume and void radii decrease as the density increases. Based on the analysis of simplex statistics, the perfect tetrahedron AlO_4 (PTE) was determined. These PTEs may connect to each other via common oxygen to create a large poly-PTE. The largest poly-PTE consists of 19.2% Al in the sample with the lowest density and 3.8% Al in one with the highest density. From deformation of samples, elastic moduli and Poisson ratio were determined. The Young's modulus and yield stress increase with the increasing density. The strain hardening becomes more pronounced as the density increases.

1. Introduction

Amorphous alumina (a-Al_2O_3) systems have been being materials of great technological applications such as gate microelectronic devices, wear-resistant coatings, adsorbents, catalyst and corrosion science [1–5]. They have been produced by several techniques such as vapor deposition [6], anoxidation [7,8], evaporative decomposition of solution [9], electrohydrodynamic atomization [10], arc plasma cathodic [11] and rf magnetron sputtering [12,13]. These experiments indicated that the density of a-Al_2O_3 varies over a large range between 2.1 and 3.5 g cm^{-3}. The local atomic structures of a-Al_2O_3 films were determined from X-ray and neutron diffraction [7,8], extended X-ray absorption fine structures (EXAFS) [14], electron extended energy loss fine structure (EXELFS) [15], and solid-state NMR experiments [13]. According to their measurements, the Al–O bond length varies in the range from 1.8 to 1.9 Å and the Al coordination number is estimated from 4 to 6. Different models for a-Al_2O_3 have been constructed by classical molecular dynamics (MD) [16–23] and ab initio MD [24,25]. The simulations have performed on the a-Al_2O_3 models at various densities changed from low-density with four-coordinated aluminum (Al) to high-density with six-coordinated Al. The Al–O bond length of models changes from 1.74 to 1.8 Å. Considering the Al–O–Al bond angle, these models have shown a wide range of values from 93° to 130.3°. For O–Al–O bond angle they have shown that, at high density, it has the peak at 75° and the peak shifts toward larger value of 107° ± 3° when density decreases. Although a-Al_2O_3 systems with various densities have intensively studied by both experiments and simulations, many of its aspects are still not specified; for instance, the variation of bond angle distributions (BADs) and coordination numbers upon compression is not fully understood. The information on the atomic configuration with respect to BAD and coordination number is essential in the interpretation of the physical and chemical properties, such as identifying binding sites on the surface of a-Al_2O_3 catalytic supports [17], vibrational properties [25], photoemission binding energies and NMR chemical shifts [24].

The mechanical properties of a-Al_2O_3 systems have been studied by both experiments [26–29] and simulations [22,25]. These experiments and simulations have shown that the elastic moduli depend on the atomic configuration. The Young's modulus obtained from simulations is higher than that measured by experiments because of the model structure is non-porous and homogeneous [25]. However, the deformation on the local atomic structures of a-Al_2O_3 systems at a large strain has not been observed yet.

Therefore, the purpose of this work is to study the structural correlation based on the BAD and structural units AlO_x ($x = 4,5,6$) and linkage OAl_y ($y = 2,3,4$). The uniform and uniaxial deformations on a-Al_2O_3 systems are carried out. Void volume and void radii of the systems have been calculated. The analysis of simplex

* Corresponding author. Tel.: +84 4 38681572; fax: +84 4 38693498.
E-mail address: vinh.levan@hust.edu.vn (V.-V. Le).

0927-0256/$ - see front matter © 2013 Elsevier B.V. All rights reserved.
http://dx.doi.org/10.1016/j.commatsci.2013.06.019

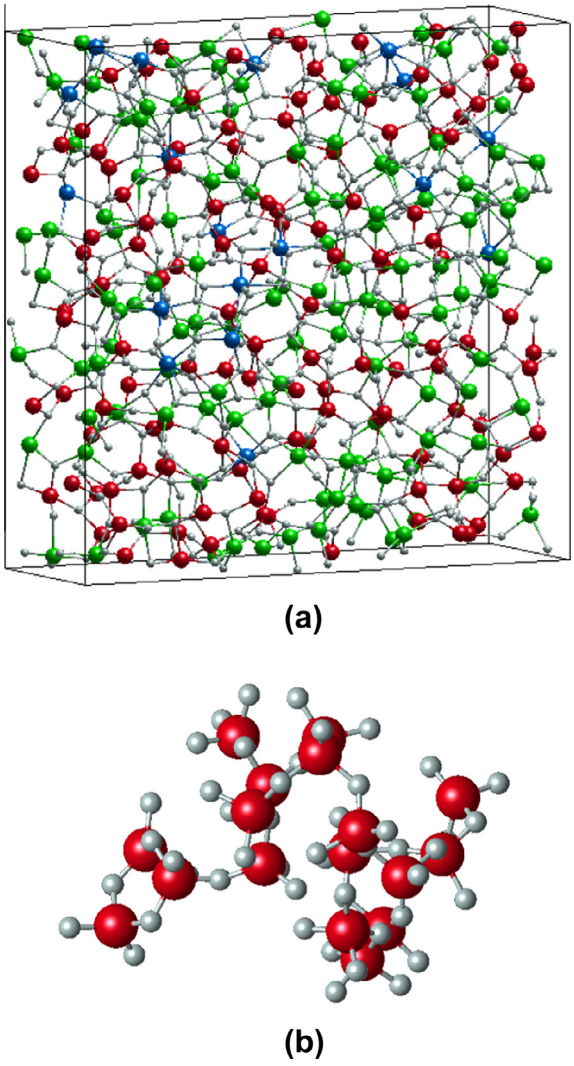

Fig. 1. (a) The structure of the central region (red: Al_4, green: Al_5 and blue: Al_6) and (b) a poly-PTE in the sample M3 (large and small spheres represent Al and O, respectively). (For interpretation of the references to color in this figure legend, the reader is referred to the web version of this article.)

statistics has also been used to study the local atomic structures of a-Al_2O_3 systems.

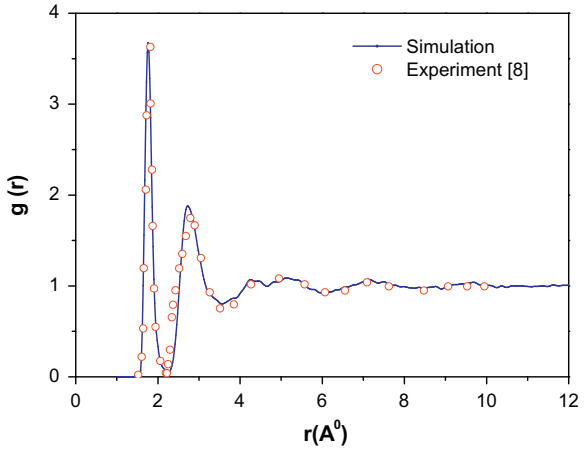

Fig. 2. The total PRDFs of a-Al_2O_3 at the density of 3.13 g cm^{-3} and experimental data [8].

2. Computational procedure

The choice of force fields to describe the interatomic interactions is essential in MD simulation. It is important to take accounts of covalent components in the simulation of the structure and properties of oxides [18]. The covalent interaction is described in terms of three-body interaction potential [22], which significantly increases the computational time. Therefore, the models should be simplified. Here, we have used the pair potential of Matsui [30], which has been demonstrated to reproduce a number experimental properties such as structure, density, bulk modulus, thermal expansivities, and melting temperatures [16].

The pairwise potential used here is of the form:

$$\phi_{ij} = \frac{q_i q_j e^2}{r_{ij}} + D(B_i + B_j)\exp\left(\frac{A_i + A_j - r_{ij}}{B_i + B_j}\right) - \frac{C_i C_j}{r_{ij}^6}, \quad (1)$$

where the terms represent Coulomb, repulsion and van der Waals energies, respectively. Here r_{ij} is the distance between an ion of type i and an ion of type j (i,j = Al,O), e is the elementary charge, and q_{Al} = 1.4175 and q_O = −0.9450 are effective partial charges. D is a standard force constant 4.184 kJ Å^{-1} mol^{-1}. The repulsive radius A, the softness parameter B and the van der Waals coefficients C can be found elsewhere [30,31]. The long-range Coulomb interactions were calculated with the Ewald summation technique.

Table 1
Structural characteristics of amorphous alumina (r_{xy} – position of first peak of PRDF $g_{xy}(r)$; Z_{xy} – the mean coordination number; and Al_x, O_y – the fraction of structural unit AlO_x and linkage OAl_y).

	M1	M2	M3	M4	M5	M6	Class. MD		Ab.MD	Exp.	
ρ (g cm^{-3})	2.84	3.13	3.34	3.52	3.70	3.81	2.83[19]	3.0 [16]	2.9 [24]	– [8]	– [13]
ρ_f (g cm^{-3})	2.85	3.10	3.34	3.55	3.68	3.81					
Z_{Al-O}	4.19	4.38	4.56	4.75	4.92	5.07	4.48	4.25	4.44	4.10	4.48
Z_{O-Al}	2.81	2.92	3.04	3.16	3.26	3.34	2.98	2.83	–	–	–
r_{Al-Al} (Å)	3.14	3.12	3.10	3.08	3.06	3.02	3.22	3.12	3.20	3.20 ± 0.55	–
r_{Al-O} (Å)	1.76	1.76	1.76	1.76	1.76	1.78	1.78	1.76	1.85	1.80 ± 0.21	–
r_{O-O} (Å)	2.76	2.74	2.72	2.68	2.66	2.60	2.81	2.75	2.75	2.80 ± 0.58 –	
$\langle\theta_{O-Al-O}\rangle$	106°	103°	96°	92°	89°	88°	107°	104°	104.12°	–	–
$\langle\theta_{Al-O-Al}\rangle$	120°	120°	121°	121°	120°	115°	125°	120°	120°	125°	–
Al_4	0.787	0.639	0.496	0.360	0.274	0.189	0.54	0.85	0.48	0.56	0.55 ± 0.03
Al_5	0.200	0.326	0.443	0.518	0.530	0.547	0.44	0.13	0.43	0.22	0.42 ± 0.03
Al_6	0.008	0.033	0.060	0.121	0.196	0.264	0.02	0.06	0.04	–	0.03 ± 0.02
O_2	0.217	0.146	0.083	0.034	0.027	0.014	–	0.25	–	–	–
O_3	0.758	0.781	0.795	0.759	0.669	0.600	–	0.74	–	–	–
O_4	0.024	0.072	0.122	0.204	0.301	0.379	–	0.01	–	–	–
β	0.145	0.132	0.120	0.109	0.101	0.095					
γ	0.382	0.351	0.325	0.299	0.282	0.268					